Journal of Magnetism and Magnetic Materials 475 (2019) 70–75

Contents lists available at ScienceDirect

Journal of Magnetism and Magnetic Materials

journal homepage: www.elsevier.com/locate/jmmm

Research articles

Nanoscale modification of magnetic properties for effective domain wall pinning

Tianli Jin[a], Funan Tan[a], Wai Cheung Law[a], Weiliang Gan[a], Ivan Soldatov[b,e], Rudolf Schäfer[b,c], Chuang Ma[d], Xiaoxi Liu[d], Wen Siang Lew[a], S.N. Piramanayagam[a,*]

[a] Division of Physics and Applied Physics, School of Physical and Mathematical Sciences, Nanyang Technological University, 637371, Singapore
[b] Leibniz Institute for Solid State and Materials Research (IFW) Dresden, Institute for Metallic Materials, Helmholtzstrasse 20, D-01069 Dresden, Germany
[c] Institute for Materials Science, TU Dresden, 01062 Dresden, Germany
[d] Department of Electrical and Computer Engineering, Shinshu University, Wakasato 4-17-1, Nagano 380-8553, Japan
[e] Institute of Natural Sciences, Ural Federal University, 620002 Ekaterinburg, Russia

A B S T R A C T

Magnetic domain wall memory technology, wherein the information is stored in magnetic domains of multiple magnetic nanowires, is a potential concept proposed to store the large amount of digital data in the near future, which is generated due to the widespread use of social media and computing devices. However, one of the technological challenges which remains to be solved in domain wall memory is the controllable pinning of the domain walls at the nanometer scale. Here, we demonstrate the possibility to stabilize domain walls with nanoscale modification of magnetic properties by using thermal diffusion of elements from crossbar configuration. We have inspected and evaluated the magnetic properties of the nanowires using Kerr microscopy. The pinning field induced by Cr diffusion of our $Ni_{80}Fe_{20}$ nanowire was estimated to be about 8 kA/m as determined from minor loop (magnetoresistance vs. magnetic field) measurements. The proposed concept can potentially be used in future domain wall memory applications.

Spintronic-based devices have gained much attention within the past few years [1–3]. Devices such as magnetic random access memory (MRAM) show promise in embedded memory applications, for temporary storage of a few gigabytes [2]. On the other hand, domain wall (DW) based devices, which hold multiple bits, are promising candidates for high-density, non-volatile information storage [4,5]. Information in these devices are stored in the states of domain magnetization similar to a hard disk drive, while for "reading" the stored information in the domain wall memory devices is always extracted by moving domains along the wire instead of operation with an actuator and motor. DW devices enable high capacity, when DW nanowires are stacked in three dimensions. All this, together with high DW velocity of 750 m/s reported in Ref. [6], DW memory shows excellent potential for information storage. However, one of the challenges associated with a domain wall memory is to write and move domains precisely. It is well known that the magnetic field used to generate domains could cause a stochastic spread over a large distance of several micrometers. The stochastic behavior limits the density of information storage [7–12]. Therefore, it is essential to control the domain wall motion by pining domain walls precisely in order to make the operation of domain wall devices reliable and to achieve higher capacity [4,5,13].

As domain walls are stabilized by pinning sites (energy barriers or potential wells), an artificial method of forming pinning sites is a useful way to control DW propagation [7,9,14]. Until now, the pinning sites for domain wall devices are fabricated by complicated lithography processes, such as the creation of notches in the ferromagnetic nanowire as shown in Fig. 1(a) [15–19]. With this technique, however, the pinning effect could be non-uniform due to shape and size variations, indicating that better solutions are desired. Another problem of notches in the nanowire is the fact that they cause a reduction of the wire lateral dimensions, leading to an increased local heating at the notch position. In addition, if the notches are made using the lowest limits of the lithography technique (the notch with a depth of F), the width of domain wall nanowires tend to be bigger (2F–3F) and hence there is a compromise in the areal density of nanowires. Therefore, better techniques to pin the domain walls are desired [20].

In this paper, we propose an alternative efficient method to precisely pin domain wall positions by a local modification of the magnetic properties of the nanowire (Fig. 1(b)). The local modification is achieved by heat-induced diffusion of a suitable element from a crossbar configuration into the magnetic nanowire. Firstly, we carried out simulations to investigate if the domain walls could be stabilized by local compositional variation. Then, we carried out magnetic property measurements at the thin film level to verify the effectiveness of tuning the properties of Permalloy ($Ni_{80}Fe_{20}$) by using metal diffusion. Ultimately, $Ni_{80}Fe_{20}$ (NiFe) nanowires were fabricated as domain wall

* Corresponding author.
E-mail address: prem@ntu.edu.sg (S.N. Piramanayagam).

https://doi.org/10.1016/j.jmmm.2018.11.114
Received 8 October 2018; Received in revised form 13 November 2018; Accepted 24 November 2018
Available online 24 November 2018
0304-8853/

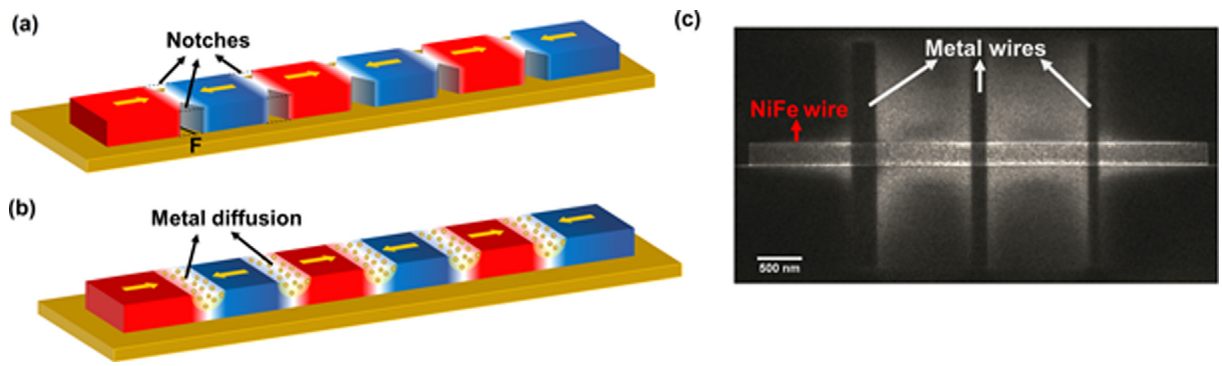

Fig. 1. Conventional pinning method, which utilize physical notches to pin domain walls (a). Proposed non-topographical method of using nanoscale modification of magnetic properties to pin domain walls (b). A NiFe nanowire with metal wires crossbars to modify the magnetic properties by metal diffusion (c).

devices, which were partially covered with a metallic capping layer to form a crossbar structure as shown in Fig. 1(c). The pinning process was observed by Wide-field Kerr microscopy [21,22], which was performed on nanowires without or with metallic capping layer. Magnetoresistance (*MR*) measurements were carried as a function of applied field (*H*), including the recording of minor *MR-H* loops, to monitor the pinning strength.

For the micro-magnetic simulation studies, the material parameters were chosen based on the literature data of NiFe nanowires (saturation magnetization M_s of 880 kA/m, exchange stiffness A of 13×10^{-12} J/m, Gilbert damping constant α of 0.008, and a zero anisotropy energy) [23]. For the magnetically modified region, representing the pinning site, the following parameters were used: saturation magnetization M_s of 430 kA/m, exchange stiffness A of 6.5×10^{-12} J/m and a larger damping constant of 0.024. The simulated nanowire has a length of 512 nm, a width of 128 nm, and a thickness of 10 nm. Firstly, one transverse domain wall was introduced and was relaxed as shown in Fig. 2(a). Fig. 2(b)–(e) show the snapshot images of the propagating wall in the nanowire without pinning site by sending current at a density $J = 1.9 \times 10^{12}$ A/m^2, which is driven by spin transfer torque. After 3 ns, the domain wall has moved to the right and then disappeared at the right side of nanowire. When the NiFe nanowire has a modified region with a length of 100 nm, as shown in Fig. 2(f), the domain wall gets pinned at the modified region, as shown in Fig. 2(g)–(j). In less than 3 ns, the domain wall has moved to the modified region, driven by a current with a density of $J = 1.9 \times 10^{12}$ A/m^2. Even after 10 ns, the wall still remains pinned at the modified region. These simulation results show that the domain walls can be effectively pinned at compositionally modified regions, acting as pinning centres, which indicates that the proposed scheme has the potential to pin domain walls in a controllable manner.

In order to verify the pinning effect experimentally, we deposited

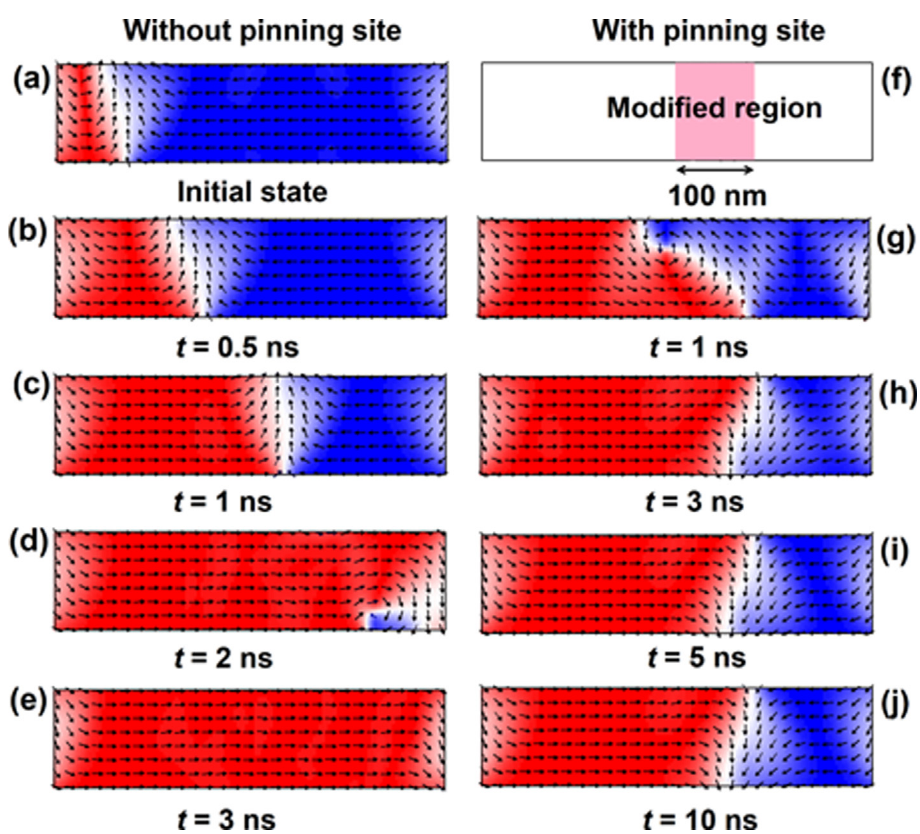

Fig. 2. Simulated domain wall propagation along the homogenious (a–e) and locally modified (f–j) nano-wire with length of 512 nm under the charge current applied with initial wall position (a). The NiFe nanowire has the modified region with length of 100 nm.

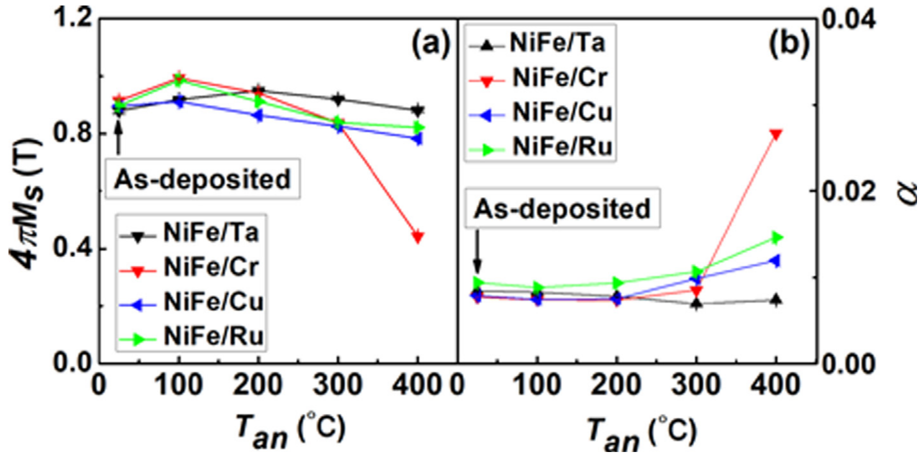

Fig. 3. Effective saturation magnetization $4\pi M_s$ as a function of annealing temperature (a). Damping constant α as a function of annealing temperature for different metallic capping layer (b).

10 nm thick NiFe thin films with different metallic capping layers. Fig. 3(a) and (b) show the static and dynamic magnetic properties of the $Ni_{80}Fe_{20}$ (10 nm)/X (5 nm) samples, such as effective saturation magnetization $4\pi M_s$ and damping constant α at different annealing temperature (T_{an}). Here, X refers to the metallic capping layers including Ta, Cr, Cu and Ru [24,25]. For as-deposited $Ni_{80}Fe_{20}$, the saturation magnetization $4\pi M_s$ is about 0.886 T at room temperature [26,27]. The effective saturation magnetization $4\pi M_s$ decreases with increasing T_{an} from 100 to 400 °C for all metallic capping layers. The decrease is most significant in the case of Cr, where $4\pi M_s$ drops to 0.427 ± 0.009 T at T_{an} = 400 °C. For copper capping layer, $4\pi M_s$ decreases from 0.878 ± 0.003 T to 0.768 ± 0.006 T after 400 °C annealing. For Ta and Ru, the magnetization decreases at a much slower rate. $Ni_{80}Fe_{20}$ has a small Gilbert damping constant α of 0.008 in the as-deposited state [26]. The damping constant shows an increase after annealing for all capping materials. For a Cu capping layer, the damping constant α of the annealed films increases to 0.012, and for a Ru capping layer, it increases to 0.011at T_{an} = 400 °C. The influence of a Ta capping layer is negligible. For Cr, an increase of the damping constant α to 0.024 is observed, which corresponds to an increase of almost 250% at T_{an} = 400 °C. The investigations discussed so far have demonstrated that Cr has the strongest effect in changing both the static ($4\pi M_s$) and dynamic (α) properties of our $Ni_{80}Fe_{20}$ film and can be chosen for further experiments.

In order to study the pinning effect introduced by Cr-modified crossbars, we carried out Kerr imaging on the nanowires at different applied magnetic fields. Fig. 4(a) shows images which were taken at different fields for wires with a width of 4 μm. It can be noticed that the domain wall propagation is stochastic. The domain wall shows rapid propagation between 1.03 kA/m and 1.27 kA/m. Fig. 4(b) shows the domain patterns in 1 μm wires without crossbars and Fig. 4(c) shows the images for wires with crossbars. It can be noticed from Fig. 4(b) that the domain wall propagation is random in the case of wires without Cr crossbars. For samples with Cr crossbars, the domains appear to nucleate at the pinning sites and then propagate. This is a typical problem associated with field-dependent domain wall motion investigations where the whole wire is subject to a field. Nevertheless, hysteresis loops of the two wires were measured by extracting the intensity of the wire region and they are shown in Fig. 4(d) and (e). In all the measurements of Fig. 4, the field was applied along the length of the wire. An obvious increase in the coercivity is observed in samples with Cr crossbars, indicating an additional energy barrier for domain wall propagation. However, no direct evidence was found in the images 4(b) and (c) to verify a clear sign for domain wall pinning due to the Cr crossbar.

In order to have a better understanding on the domain wall motion, we carried out magnetoresistance measurements of the devices. NiFe nanowires, as shown in Fig. 5(a) and (b), were fabricated for this purpose. A DC current (I) of 30 μA was applied through the nanowires. At the same time, a nanovoltmeter was used to pick up the voltage. Fig. 5(c) shows the resistance (R) versus applied magnetic field (H) curve for the pure NiFe sample. When the magnetic field H is parallel to the direction of I, we can observe that the magnetoresistance is high. The change in R-H is negligible in the case of the nanowire without artificial pinning sites. For magnetic field H direction perpendicular to the current I ($H \perp I$), a change in resistance of about 1.5% was observed. These results are typical properties of $Ni_{80}Fe_{20}$ and these results validate the fabrication process of the nanowires [27].

Fig. 5(d) shows the R-H curve for NiFe wires with Cr crossbars. The behavior of the curve for $H \perp I$ is similar to that of $Ni_{80}Fe_{20}$ without Cr crossbars. The magnitude of change in R-H is about 0.8%, which is lower thus indicating the effect of Cr diffusion. However, we can notice a striking difference in the R-H for the case $H||I$, where a dip at fields of about 8 kA/m is seen. This is not a common feature of NiFe and hence we can safely say that this effect is brought out by the Cr crossbars. It is expected that the pinning centres lead to the presence of an energy barrier at every pinning site. If there is an energy barrier associated with the pinning sites (Cr-diffused regions), then the R-H curves should exhibit an irreversible behavior. To categorically observe such an irreversible behavior, minor R-H curves were measured. The magnetic field was swept starting from a saturated state (48 kA/m) to reversal fields (H_{Re}), such as −4 kA/m, −5.57 kA/m, −7.16 kA/m and −8.75 kA/m, and then returned back to the saturated state at 48 kA/m. Fig. 6(a–d) show the reversal curves for different H_{Re}. A kind of hysteresis in the R-H curves is observed and the area occupied by the curves (Fig. 6(e)) increased. A R-H curve, similar to Fig. 5(d) has been reported in the study of Mohanan et al. [18], where the resistance of $Ni_{80}Fe_{20}$ nanowire drops due to domain wall injected by a junction pad and pinned by notches. The depinning field was about 6.4 kA/m in their study [18]. However, they did not report a minor R-H loop as carried out in our study. Similar to the area in a B-H loop, the areas of these curves indicate the energy required to overcome the pinning strength of the domain walls [28,29]. The points marked in the figures correspond to different domain configurations, as shown the inset. These results indicate that the Cr diffused regions indeed act as pinning centers.

To summarize, a new domain wall pinning method using local compositional modifications is proposed and examined theoretically and experimentally. Micromagnetic simulation predicts the ability of local modification to increase pinning on desired positions. Diffusion of Cr among other metals proved to be more effective in changing the magnetic static and dynamic properties. R-H curves show that the Cr crossbars help to pin the domain walls. Although the annealing effect on the magnetic properties of NiFe and NiFe coated with Cr is

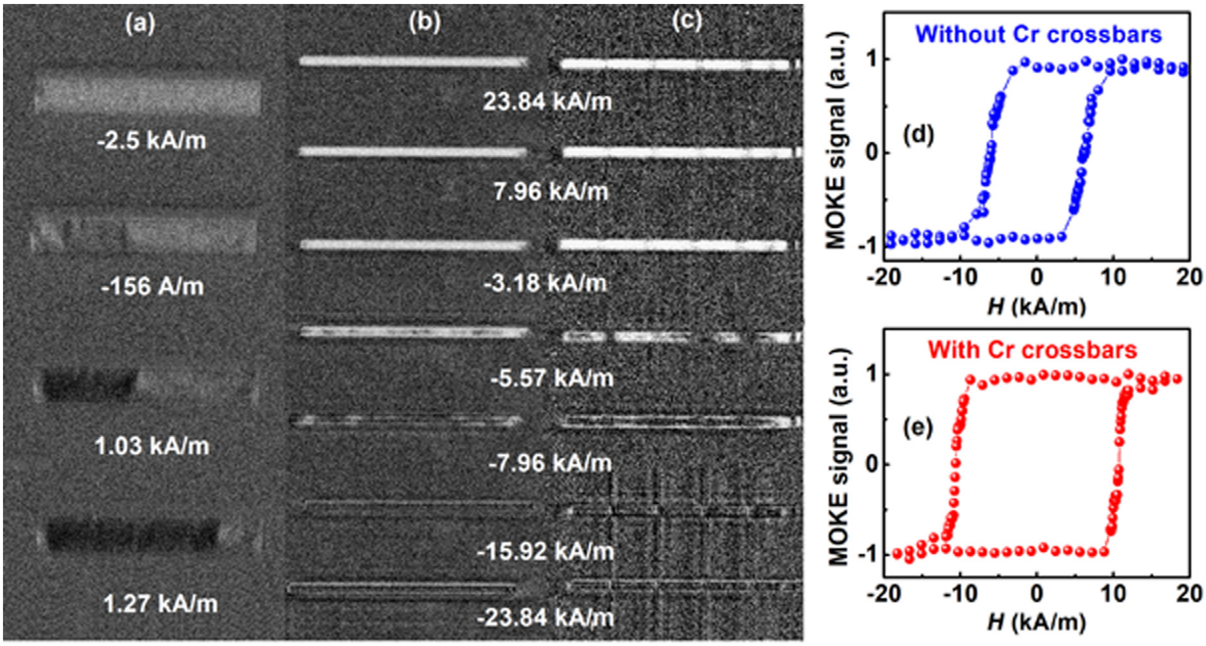

Fig. 4. High-resolution Kerr images of domain evaluation in an external magnetic field on NiFe wire (4 µm width) (a), 1 µm width without metal wire (b) and with Cr wire (c), imaged with a 100× oil immersion lens. In-plane magneto optical loops measured on NiFe wires without capping metal crossbar (d) and with Cr crossbar (e).

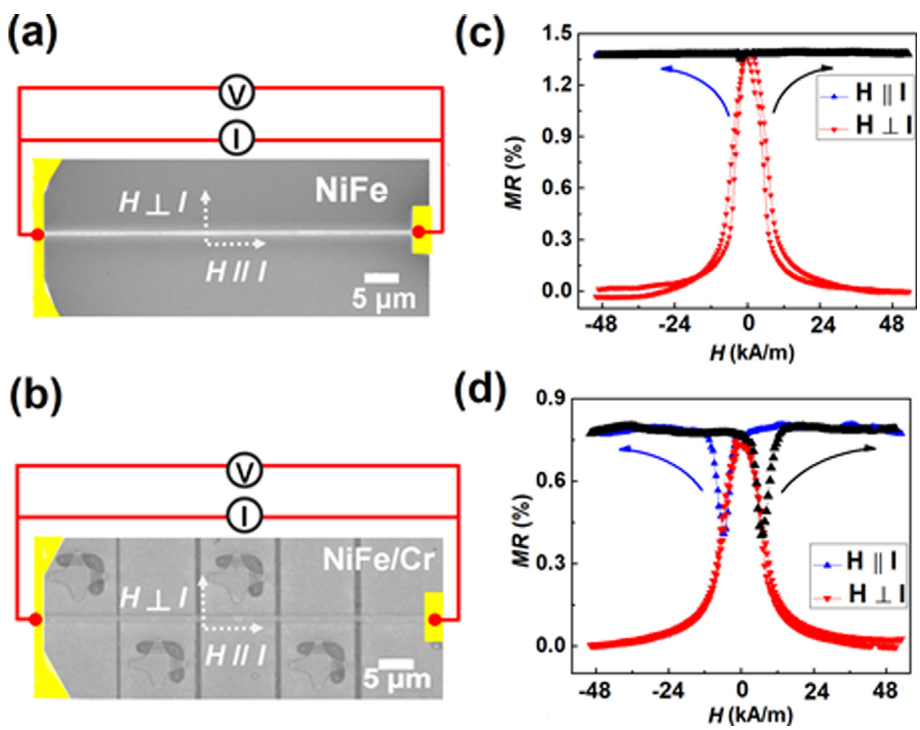

Fig. 5. Optical image with schematics of NiFe wires and the electrodes without (a) and with Cr crossbars (b). Change of resistance in NiFe wires without (c) and with (d) Cr crossbars as a function of magnetic field.

investigated experimentally in this study, compositional modification can also be carried out using techniques such as ion-implantation [30,31]. For much higher density operation, materials with a perpendicular magnetic anisotropy may be used.

1. Methods

All the $Ni_{80}Fe_{20}$ film without capping layer and with capping layers were deposited by using dc magnetron sputtering at room temperature. The base pressure of the sputtering chamber was lower than 1.1×10^{-7} Torr. The argon pressure during the deposition of $Ni_{80}Fe_{20}$ layer was fixed at 2 mTorr and the sputter power was 40 W. $Ni_{80}Fe_{20}$ films with capping layers were annealed for 1 h at different T_{an} from 100 °C to 400 °C in vacuum condition with base pressure below 5×10^{-7} Torr. Alternating Gradient Force Magnetometry (AGFM) and broad band Ferromagnetic resonance (FMR) spectroscopy was used to obtain the measurements to obtain the magnetic properties.

The NiFe and Cr nanowires were fabricated by E-beam lithography

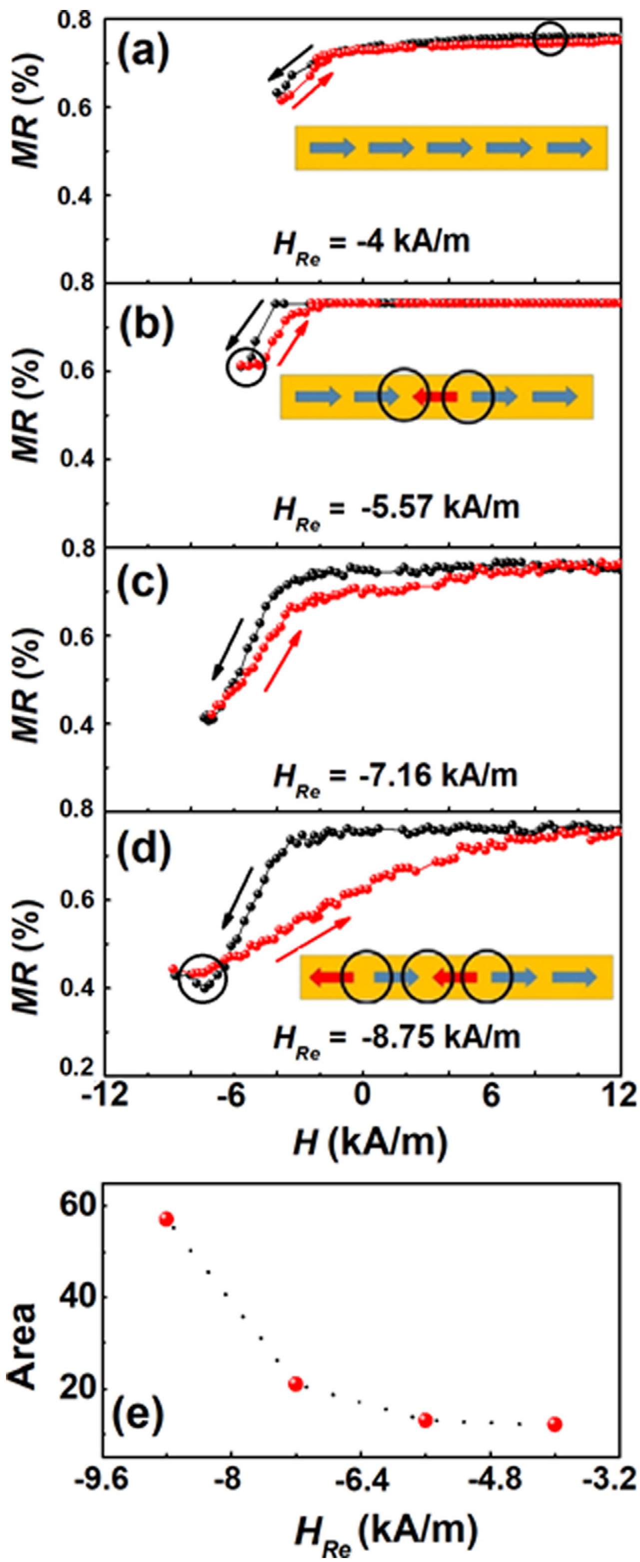

Fig. 6. Minor loop measurement of the *R-H* curves, starting from a saturation field, to a reversal field H_{Re} and back to saturating field. (a)–(d) are the minor resistance-field hysteresis loops for different reversal fields, H_{Re}. The inset shows the points marked in the loops that correspond to different domain configurations as illustrated by the arrows. The area occupied by the curves for different reversal fields are plotted in (e).

(EBL). The first layer of resist over the NiFe film was exposed under 20 kV voltage and 7 μm aperture. After E-beam exposure, Argon ion-milling was carried out to eliminate the unwanted film. The second layer of resist over NiFe wires was exposed under 10 kV voltage and 30 μm aperture. After developing to remove the resist which has been exposed by E-beam, Cr was deposited in the holes of the second layer of resist. The NiFe sample with Cr crossbars was annealed at 400 °C for one hour in a vacuum chamber to make Cr diffusion into the NiFe nanowire at the cross section to form pinning sites.

Acknowledgements

We gratefully acknowledge Nanyang Technological University Start-Up Grant, AcRF-Tier 1 grant RG163/15 of Ministry of Education Singapore, and NTU-JSPS grant offered by Nanyang Technological University, Singapore and Japan Society for the Promotion of Science for the funding and support of this research.

Appendix A. Supplementary data

Supplementary data to this article can be found online at https://doi.org/10.1016/j.jmmm.2018.11.114.

References

[1] R. Sbiaa, S.N. Piramanayagam, Recent developments in spin transfer torque MRAM, Phys. Status Solidi RRL 11 (2017) 1700163.
[2] S. Bhatti, R. Sbiaa, A. Hirohata, H. Ohno, S. Fukami, S.N. Piramanayagam, Spintronics based random access memory: a review, Mater. Today 20 (2017) 530–548.
[3] J.S. Meena, S.M. Sze, U. Chand, T.Y. Tseng, Overview of emerging nonvolatile memory technologies, Nanoscale Res. Lett. 9 (2014) 526.
[4] S.S.P. Parkin, M. Hayashi, L. Thomas, Magnetic domain-wall racetrack memory, Science 320 (2008) 190–194.
[5] S. Parkin, S.H. Yang, Memory on the racetrack, Nat. Nanotechnol. 10 (2015) 195–198.
[6] S.H. Yang, K.S. Ryu, S. Parkin, Domain-wall velocities of up to 750 m s(-1) driven by exchange-coupling torque in synthetic antiferromagnets, Nat. Nanotechnol. 10 (2015) 221–226.
[7] S. Parkin, X. Jiang, C. Kaiser, A. Panchula, K. Roche, M. Samant, Magnetically engineered spintronic sensors and memory, Proc. IEEE 91 (2003) 661–680.
[8] S.S.P. Parkin, Data in the fast lanes of racetrack memory, Sci. Am. 300 (2009) 76–81.
[9] W.S. Zhao, Y. Zhang, H.P. Trinh, J.O. Klein, C. Chappert, R. Mantovan, A. Lamperti, R.P. Cowburn, T. Trypiniotis, M. Klaui, J. Heinen, B. Ocker, D. Ravelosona, Magnetic Domain-Wall Racetrack Memory for high density and fast data, Storage (2012).
[10] R.L. Stamps, S. Breitkreutz, J. Akerman, A.V. Chumak, Y. Otani, G.E.W. Bauer, J.U. Thiele, M. Bowen, S.A. Majetich, M. Klaui, I.L. Prejbeanu, B. Dieny, N.M. Dempsey, B. Hillebrands, The 2014 magnetism roadmap, J. Phys. D Appl. Phys. 47 (2014).
[11] S.N. Piramanayagam, Perpendicular recording media for hard disk drives, J. Appl. Phys. 102 (2007) 011301.
[12] S.N. Piramanayagam, B. Varghese, H.K. Tan, Y.Y.K. Hnin, W.K. Lee, I. Okamoto, L.J. Wu, D. Tripathy, Writability improvement in perpendicular recording media using crystalline soft underlayer materials, IEEE Trans. Magn. 49 (2013) 758–764.
[13] I. Polenciuc, A.J. Vick, D.A. Allwood, T.J. Hayward, G. Vallejo-Fernandez, K. O'Grady, A. Hirohata, Domain wall pinning for racetrack memory using exchange bias, Appl. Phys. Lett. 105 (2014) 162406.
[14] D. Atkinson, D.S. Eastwood, L.K. Bogart, Controlling domain wall pinning in planar nanowires by selecting domain wall type and its application in a memory concept, Appl. Phys. Lett. 92 (2008) 022510.
[15] L.K. Bogart, D. Atkinson, K. O'Shea, D. McGrouther, S. McVitie, Dependence of domain wall pinning potential landscapes on domain wall chirality and pinning site geometry in planar nanowires, Phys. Rev. B 79 (2009).
[16] S.H. Huang, C.H. Lai, Domain-wall depinning by controlling its configuration at notch, Appl. Phys. Lett. 95 (2009).
[17] T.J. Hayward, K.A. Omari, Beyond the quasi-particle: stochastic domain wall dynamics in soft ferromagnetic nanowires, J. Phys. D Appl. Phys. 50 (2017) 084006.
[18] V.P. Mohanan, P.S.A. Kumar, Chirality dependent pinning and depinning of magnetic vortex domain walls at nano-constrictions, J. Magn. Magn. Mater. 422 (2017) 419–424.
[19] A.J.V.I. Polenciuc, D.A. Allwood, T.J. Hayward, G. Vallejo-Fernandez, K. O'Grady, A. Hirohata, Appl. Phys. Lett. 105 (2014) 162406.
[20] T. Jin, D. Kumar, W. Gan, M. Ranjbar, F. Luo, R. Sbiaa, X. Liu, W.S. Lew, S.N. Piramanayagam, Nanoscale compositional modification in Co/Pd multilayers for controllable domain wall pinning in racetrack memory, Phys. Status Solidi RRL (2018).
[21] D. Markó, I. Soldatov, M. Tekielak, R. Schäfer, Stray-field-induced Faraday contributions in wide-field Kerr microscopy and- magnetometry, J. Magn. Magn. Mater. 396 (2015) 9–15.
[22] I.V. Soldatov, R. Schäfer, Advances in quantitative Kerr microscopy, Phys. Rev. B 95

(2017).
[23] D.W. Wong, I. Purnama, G.J. Lim, W.L. Gan, C. Murapaka, W.S. Lew, Current-induced three-dimensional domain wall propagation in cylindrical NiFe nanowires, J. Appl. Phys. 119 (2016).
[24] A. Hirohata, K. Takanashi, Future perspectives for spintronic devices, J. Phys. D Appl. Phys. 47 (2014).
[25] B. Marchon, T. Pitchford, Y.T. Hsia, S. Gangopadhyay, The head-disk interface roadmap to an areal density of 4 Tbit/in(2), Adv. Tribol. (2013).
[26] T.L. Jin, M. Ranjbar, S.K. He, W.C. Law, T.J. Zhou, W.S. Lew, X.X. Liu, S.N. Piramanayagam, Tuning magnetic properties for domain wall pinning via localized metal diffusion, Sci. Rep. 7 (2017).
[27] Y.L. Yin, F. Pan, M. Ahlberg, M. Ranjbar, P. Durrenfeld, A. Houshang, M. Haidar, L. Bergqvist, Y. Zhai, R.K. Dumas, A. Delin, J. Akerman, Tunable permalloy-based films for magnonic devices, Phys. Rev. B 92 (2015).
[28] P.K. Budig, Magnetic bearings with DC bias: design and optimum, Mater. Choice (2008).
[29] S.N. Piramanayagam, M. Ranjbar, R. Sbiaa, C.T. Chong, Magnetic and first-order reversal curve investigations of antiferromagnetically coupled nanostructures of Co/Pd multilayers, IEEE Trans. Magn. 48 (2012) 3410–3413.
[30] D.M. Burn, D. Atkinson, Control of domain wall pinning by localised focused Ga + ion irradiation on Au capped NiFe nanowires, J. Appl. Phys. 116 (2014) 163901.
[31] N. Gaur, K.K.M. Pandey, S.L. Maurer, S.N. Piramanayagam, R.W. Nunes, H. Yang, C.S. Bhatia, Magnetic and structural properties of CoCrPt-SiO2-based graded media prepared by ion implantation, J. Appl. Phys. 110 (2011) 083917.